Journal of Physics: Conference Series **3053** (2025) 012006 doi:10.1088/1742-6596/3053/1/012006

# Velocity decorrelation functions of high-energy cosmic rays propagating in magnetic fields

**Olivier Deligny**[1]

[1]Laboratoire de Physique des 2 Infinis Irène Joliot-Curie (IJCLab)
CNRS/IN2P3, Université Paris-Saclay, Orsay, France

E-mail: deligny@ijclab.in2p3.fr

**Abstract.** Diffusion tensor coefficients play a central role in describing cosmic ray transport in various astrophysical environments permeated with magnetic fields, which are usually modeled as a fluctuating field on top of a mean field. In this contribution to CRIS-MAC 2024, a formal derivation of these coefficients is presented by means of the calculation of velocity decorrelation functions of particles. It relies mainly on expanding the 2-pt correlation function of the (fluctuating) magnetic field experienced by the particles between two successive times in the form of an infinite Dyson series and retaining a class of terms that converge to a physical solution. Subsequently, the velocity decorrelation functions, themselves expressed as Dyson series, are deduced from an iteration procedure that improves on the partial summation scheme. The results are shown to provide approximate solutions compared to those obtained by Monte-Carlo simulations as long as the Larmor radius of the particles is larger than at least one tenth of the largest scale of the turbulence.

In many astrophysical environments, the propagation and acceleration of high-energy charged particles (cosmic rays) are governed by the scattering off magnetic fields, which are described as a turbulence $\delta\mathbf{B}$ on top of a mean field $\mathbf{B}_0$. The transport of the particles is then modelled as an anisotropic diffusion process. Under very broad conditions, the coefficients of the diffusion tensor can be related to the velocity correlation function of cosmic rays, $\langle v_{0i} v_j(t)\rangle$, through a time integration [1],

$$D_{ij}(t) = \int_0^t \mathrm{d}t' \, \langle v_{0i} v_j(t')\rangle, \tag{1}$$

in the limit that $t \to \infty$. Here, $v_{0i} \equiv v_i(t=0)$[1] and $\langle\cdot\rangle$ stands for the average quantities, taken over several space and time correlation scales of the turbulent field. Many estimates of these coefficients have been made from numerical simulations exploring wide ranges of particle rigidities and turbulence levels [2, 3, 4, 5, 6, 7, 8, 9, 10, 11, 12, 13, 14, 15, 16, 17, 18, 19]. Formal estimates, on the other hand, have been presented in [9] in the high rigidity regime, and in [20, 21] in the gyro-resonant regime. In this contribution to CRIS-MAC 2024, we present these latter estimates. Without loss of generalities, the study is limited to the example of an isotropic 3D turbulence following a Kolmogorov power spectrum without helicity. The setup for the mean field is such that $\mathbf{B}_0 = B_0 \mathbf{u}_z$.

We are interested in determining the moments of $v_i(t)$ to derive a workable expression for Eqn. 1. The velocity of each test-particle is governed by the Lorentz-Newton equation of motion,

$$\dot{v}_i(t) = \delta\Omega(t)\ \epsilon_{ijk} v_j(t) \delta b_k(t) + \Omega_0\ \epsilon_{ijk} v_j(t) b_{0k}(t). \tag{2}$$

[1]Since cosmic rays are high-energy relativistic particles, the norm of the velocity is identified to $c$ for convenience.

Here, $\delta\Omega(t) = c^2 Z|e|\delta B(t)/E$ is the gyrofrequency related to the turbulence, $\Omega_0$ that related to the mean field, $Z|e|$ and $E$ the electric charge and the energy of the particle, and $\delta b_k(t) \equiv \delta b_k(\mathbf{x}(t))$ the $k$-th component of the turbulence (expressed in units of $\delta B$) at the spatial coordinate $\mathbf{x}(t)$, which corresponds to the position of the test-particle at time $t$. A formal solution for $\langle v_i(t)\rangle$ can be obtained by expressing the solution of Eqn. 2 as an infinite number of Dyson series, each combining terms in powers of $\delta\mathbf{b}$ coupled to terms in powers of $\mathbf{B}_0$. Dealing with such an infinite number of Dyson series is however hardly manageable. To circumvent this difficulty, we use the auxiliary variable introduced in [9], $w_i(t) = R_{ij}(\Omega_0 t)v_j(t)$, with $\mathbf{R}(\Omega_0 t)$ the rotation matrix of angle $\Omega_0 t$ around $\mathbf{u}_z$. The equation of motion for $\mathbf{w}$ is then

$$\dot{w}_i(t) = \delta\Omega\ R_{ij}(\Omega_0 t)\epsilon_{jk\ell}R^{-1}_{km}(\Omega_0 t)w_m(t)\delta b_\ell(t), \tag{3}$$

the formal solution of which can be expressed as a *single* Dyson series:

$$\langle w_{i_0}(t)\rangle = w_{0i_0} + \sum_{p=1}^{\infty}\delta\Omega^p\ \epsilon_{k_1m_1n_1}\epsilon_{k_2m_2n_2}\dots\epsilon_{k_pm_pn_p}w_{0i_p}\int_0^t \mathrm{d}t_1\int_0^{t_1}\mathrm{d}t_2\cdots\int_0^{t_{p-1}}\mathrm{d}t_p$$
$$\times R_{i_0k_1}(\Omega_0 t_1)R_{i_1k_2}(\Omega_0 t_2)\cdots R_{i_{p-1}k_p}(\Omega_0 t_p)R^{-1}_{m_1i_1}(\Omega_0 t_1)R^{-1}_{m_2i_2}(\Omega_0 t_2)\cdots R^{-1}_{m_pi_p}(t_p)\langle\delta b_{n_1}(t_1)\dots\delta b_{n_p}(t_p)\rangle. \tag{4}$$

In the following, we derive the velocity correlation functions, $\langle v_{0i}v_j(t)\rangle$, based on this equation.

In the Gaussian approximation, the Wick theorem allows for expressing $\langle\delta b_{n_1}(t_1)\dots\delta b_{n_p}(t_p)\rangle$ in terms of all possible permutations of products of contractions of pairs of $\langle\delta b_{n_i}(t_i)\delta b_{n_j}(t_j)\rangle$, which can be, in the case of 3D isotropic turbulence, written as

$$\langle\delta b_{n_1}(t_i)\delta b_{n_2}(t_j)\rangle = \frac{\delta_{n_1n_2}}{3}\varphi(t_i - t_j). \tag{5}$$

The correlation function $\varphi(t)$, which describes the correlation of the turbulence experienced by a test-particle along its path at two different times, follows from

$$\varphi(t) \simeq \int_{\mathbf{k}_{\min}}^{\mathbf{k}_{\max}}\mathrm{d}\mathbf{k}\frac{\mathcal{E}(k)}{4\pi k^2}\sin^2\theta_k\langle\mathrm{e}^{\mathrm{i}\mathbf{k}\cdot\mathbf{x}(t)}\rangle, \tag{6}$$

where the minimum wavenumber vector $\mathbf{k}_{\min}$ is related to the distance $L_{\max}$ over which the correlation function is non-zero (size of the largest "eddies"), while the maximum one $\mathbf{k}_{\max}$ is related to the scale $L_{\min}$ at which the dissipation rate of the turbulence overcomes the energy cascade rate, and where $\mathcal{E}(k)$ is the kinetic energy spectrum of the turbulence. The factor $\langle e^{\mathrm{i}\mathbf{k}\cdot\mathbf{x}(t)}\rangle$ is modelled as [22]

$$\langle\mathrm{e}^{\mathrm{i}\mathbf{k}\cdot\mathbf{x}(t)}\rangle \simeq \sum_{p\geq 0}(-(kc)^2)^p\int_0^t\mathrm{d}t_1\int_0^{t_1}\mathrm{d}t_2\cdots\int_0^{t_{2p-1}}\mathrm{d}t_{2p}\sum_{\text{pairings}}\prod_{\text{pairs }i<j}\mathrm{e}^{-(t_i-t_j)/\xi(k)}, \tag{7}$$

where the approximation $\langle(\mathbf{k}\cdot\mathbf{v}(t_1))(\mathbf{k}\cdot\mathbf{v}(t_2))\rangle \simeq (kc)^2\mathrm{e}^{-(t_1-t_2)/\xi(k)}$ has been used by introducing a correlation time scale $\xi$. Guided by Monte-Carlo simulations that show a longer falloff timescale for the 2-pt function of the fluctuating magnetic field for large $k$ compared to small $k$, a dependency in $(kc)^{-1}$ turns out to reproduce the main features of $\varphi(t)$ for a reduced rigidity (Larmor radius conventionally related to the turbulence only and expressed in units of the largest eddy scale $L_{\max}$) $\rho = 1$. An additional dependency in $\rho$ is introduced through $\xi(k,\rho) = A\rho^B/(kc)$; $A \simeq 1$ and $B \simeq 0.5$ are found to provide a good compromise to cover the gyroresonant and high-rigidity regimes. To evaluate the right hand side, only pairs with $j = i+1$ are retained. Under this approximation, which corresponds to summing unconnected diagrams [23], our estimate of $\langle\mathrm{e}^{\mathrm{i}\mathbf{k}\cdot\mathbf{x}(t)}\rangle$, denoted with a subscript 0, can be written in a compact non-linear manner:

$$\langle\mathrm{e}^{\mathrm{i}\mathbf{k}\cdot\mathbf{x}(t)}\rangle_0 \simeq 1 - (kc)^2\int_0^t\mathrm{d}t_1\int_0^{t_1}\mathrm{d}t_2\ \mathrm{e}^{-\frac{t_1-t_2}{\xi(k)}}\langle\mathrm{e}^{\mathrm{i}\mathbf{k}\cdot\mathbf{x}(t-t_1)}\rangle_0. \tag{8}$$

In the Laplace reciprocal space, the equation is then linear in $\mathcal{L}[\langle\mathrm{e}^{\mathrm{i}\mathbf{k}\cdot\mathbf{x}(t)}\rangle_0](s)$, which reads as

$$\mathcal{L}[\langle\mathrm{e}^{\mathrm{i}\mathbf{k}\cdot\mathbf{x}(t)}\rangle_0](s) = \frac{1+s\xi(k)}{(1+s\xi(k))s+(kc)^2\xi(k)}, \tag{9}$$

so that $\langle\mathrm{e}^{\mathrm{i}\mathbf{k}\cdot\mathbf{x}(t)}\rangle_0$ can be inferred from a numerical inverse Laplace transformation. Subsequently, we infer the partial-summation approximation for the 2-pt function of the fluctuating magnetic field experienced by a test particle as

$$\varphi(t) \simeq \frac{2(2\pi)^{2/3}\delta B^2}{3\left(L_{\max}^{2/3} - L_{\min}^{2/3}\right)}\int_{k_{\min}}^{k_{\max}}\mathrm{d}k\ k^{-5/3}\mathcal{L}^{-1}\left[\frac{1+s\xi(k)}{(1+s\xi(k))s+(kc)^2\xi(k)}\right](t). \tag{10}$$

Applying the Wick theorem, the Dyson series reads as

$$\langle w_{i_0}(t)\rangle = w_{0i_0} + \sum_{p=1}^{\infty}\left(\frac{\delta\Omega^2}{3}\right)^p w_{0i_{2p}} \int_0^t \mathrm{d}t_1 \int_0^{t_1} \mathrm{d}t_2 \cdots \int_0^{t_{2p-1}} \mathrm{d}t_{2p} \sum_{\text{pairings}} \prod_{j<\ell} \varphi(t_j - t_\ell)$$
$$\times \left( R_{i_{j-1}k_j}(\Omega_0 t_j) R_{i_{\ell-1}k_j}(\Omega_0 t_\ell) R^{-1}_{m_j i_j}(\Omega_0 t_j) R^{-1}_{m_j i_\ell}(\Omega_0 t_\ell) - R_{i_{j-1}k_j}(\Omega_0 t_j) R_{i_{\ell-1}k_\ell}(\Omega_0 t_\ell) R^{-1}_{k_\ell i_j}(\Omega_0 t_j) R^{-1}_{k_j i_\ell}(\Omega_0 t_\ell) \right), \tag{11}$$

which is the relevant equation to determine the time evolution of the auxiliary variable $\mathbf{w}(t)$ and subsequently of the particle velocity $\mathbf{v}(t) = \hat{R}^{-1}(\Omega_0 t)\mathbf{w}(t)$. To carry out a summation of the Dyson series, we resort to a two-step iteration procedure. In the first iteration, we calculate the propagator that would be accurate in the case of a 2-pt function $\varphi(t)$ approximated by a Dirac function. This approximation proves to be relevant in the high-rigidity regime in pure turbulence. It corresponds to the summation of the class of unconnected diagrams and represents the simplest partial summation scheme of the Dyson series [23]. However, this scheme leads to a non-physical solution in the case of a non-zero mean field and in the gyroresonant regime. A more physical solution is then obtained by including classes of nested and crossed diagrams in the partial summation of the Dyson series, in which the first iteration of the propagator is inserted into each ordered time. We now detail this scheme below.

The propagator obtained by retaining only unconnected diagrams is denoted as $\langle w_i(t)\rangle_0$. For the sake of clarity, we denote it with a subscript 0:

$$\langle w_i(t)\rangle_0 = 1 + \frac{\delta\Omega^2}{3}\int_0^t \mathrm{d}t_1 \int_0^{t_1} \mathrm{d}t_2 \left( R^{-1}_{ij}(2\Omega_0(t_1-t_2)) - (1+2\cos\Omega_0(t_1-t_2)) R^{-1}_{ij}(\Omega_0(t_1-t_2)) \right) \varphi(t_1-t_2)\langle w_i(t-t_1)\rangle_0, \tag{12}$$

which gives rise to a linear term for $\mathcal{L}[\langle w_i(x)\rangle_0](s)$ in the Laplace reciprocal space:

$$\mathcal{L}[\langle w_i(x)\rangle_0] = \mathcal{L}[1](s) + \frac{\delta\Omega^2}{3}\mathcal{L}[\langle w_i(x)\rangle_0](s)\mathcal{L}[1](s)\mathcal{L}\left[\left( R^{-1}_{ij}(2\Omega_0 x) - (1+2\cos\Omega_0 x) R^{-1}_{ij}(\Omega_0 x)\right)\varphi(x)\right](s). \tag{13}$$

The propagator $\langle w_i(t)\rangle_0$ is therefore obtained through a numerical inverse of Laplace transform. Throughout this study, the Stehfest algorithm is used, with Stehfest number $N = 20$ [24].

The second summation scheme accounts, in addition to unconnected diagrams, for contributions from nested and crossed diagrams that can be approximated by substituting internal double lines for zigzags. In this manner, both the nested and crossed contributions give rise to linear terms in $\mathcal{L}[\langle w_i(x)\rangle](s)$:

$$\mathcal{L}[\langle w_i(x)\rangle](s) = \frac{1}{s} + \frac{\delta\Omega^2}{3}\frac{\mathcal{L}[\langle w_i(x)\rangle](s)}{s}\mathcal{L}\left[\left[ R^{-1}_{ij}(2\Omega_0 x) - (1+2\cos\Omega_0 x) R^{-1}_{ij}(\Omega_0 x)\right]\varphi(x)\langle w_i(x)\rangle_0\right](s)$$
$$+ \left(\frac{\delta\Omega^2}{3}\right)^2 \mathcal{L}[\langle w_i(x)\rangle](s)\mathcal{L}[1](s)\mathcal{L}\Big[\Big[1 + R^{-1}_{ij}(\Omega_0(x_1+2x_2+x_3))(1+2\cos\Omega_0(x_1-x_3)) - R^{-1}_{ij}(\Omega_0(2x_1+2x_2))$$
$$- R^{-1}_{ij}(\Omega_0(2x_2+2x_3))\Big]\varphi(x_1+x_2)\varphi(x_2+x_3)\langle w_i(x_1)\rangle_0\langle w_i(x_2)\rangle_0\langle w_i(x_3)\rangle_0\Big](s). \tag{14}$$

The velocity decorrelation function relevant for the parallel diffusion corresponds to $i = j = z$ in equation 14. Denoting for convenience as $\hat{W}_i(s)$ the Laplace transform function $\mathcal{L}[\langle w_i(t)\rangle](s)$, the first iterated propagator inferred in the Laplace space reads as

$$\hat{W}_{0z}(s) = \frac{1}{s} - \frac{2\delta\Omega^2}{3}\frac{\hat{W}_{0z}(s)}{s}\mathcal{L}\left[\varphi(x)\cos\Omega_0 x\right](s), \tag{15}$$

while the iterated propagator reads as

$$\hat{W}_z(s) = \frac{1}{s} - \frac{2\delta\Omega^2}{3}\frac{\hat{W}_z(s)}{s}\mathcal{L}\left[\varphi(x)\langle w_z(x)\rangle_0\cos\Omega_0 x\right](s)$$
$$+ 2\left(\frac{\delta\Omega^2}{3}\right)^2\frac{\hat{W}_z(s)}{s}\mathcal{L}\Big[\varphi(x_1+x2)\varphi(x_2+x3)\langle w_z(x_1)\rangle_0\langle w_z(x_2)\rangle_0\langle w_z(x_3)\rangle_0\cos\Omega_0(x_1-x_3)\Big](s). \tag{16}$$

The resulting velocity decorrelation functions $\langle v_{0\parallel} v_\parallel(t)\rangle = \langle w_{0z} w_z(t)\rangle$ are shown in Fig. 1 for $\rho = 0.1$ (left panel) and different values of $B_0$ (and $\delta B = 1$ μG). For reference, results from Monte-Carlo experiments are shown as the

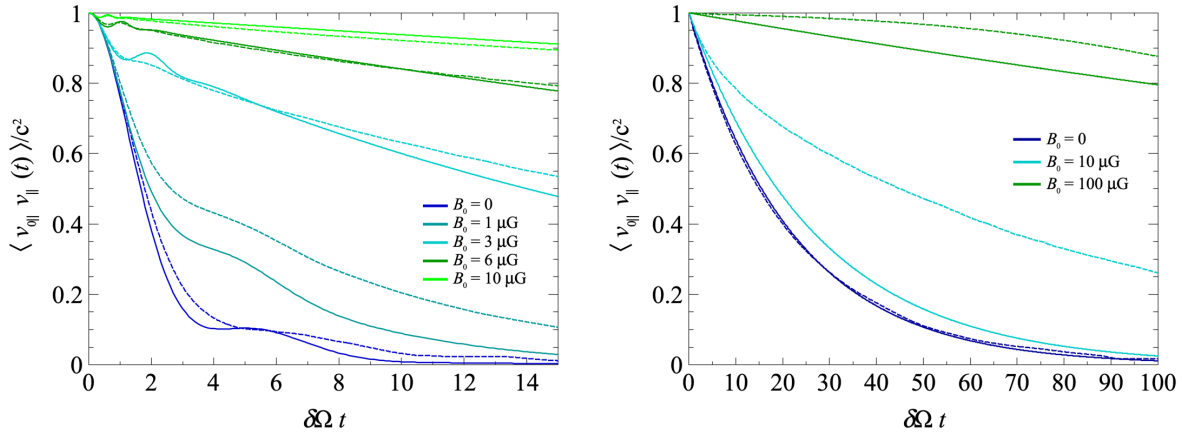


Figure 1: Parallel velocity decorrelation function of particles with reduced rigidity $\rho = 0.1$ (left) and $\rho = 1$ (right) for different values of $B_0$ ($\delta B = 1$ μG), as a function of the gyroperiod time scale $\delta\Omega t$. Dashed lines are from Monte-Carlo simulations.

dashed lines. Overall, the main features of the functions inferred from the simulations, namely the modulations on top of an approximately exponential envelope that is decreasing slower with time for increasing $B_0$ values, are captured by the calculation. In this rigidity regime, the resonance between the Larmor radius of the particles with wavelengths of the turbulence is the source of the modulations related to the total angular frequency $\delta\Omega + \Omega_0$. They reflect memory effects originating from large-scale wavenumber field lines around which particles spiral while undergoing the imprint of a random walk caused by smaller wavenumber vectors. As the intensity $B_0$ increases, the particles tend to remain bound to the lines of the mean field for longer, and the decay takes longer. Beyond similarities between the simulation and calculation results, however, quantitative differences are observed in Fig. 1. The most notable one concerns the global rate of falloff of the decorrelation functions that is predicted to be too rapid for $B_0 \lesssim 5$μG by the calculation compared to the Monte-Carlo simulations. The increase of the "decay time" describing the approximately exponential envelope is indeed too slow for small values of $B_0$, as clearly observed for $B_0 = 1$μG, before crossing the right range and getting too fast for $B_0 \gtrsim 5$μG. In other words, the dependence of the decorrelation functions in $B_0$ is non-linearly under-(over)estimated for $B_0 \lesssim (\gtrsim) 5$μG. The underestimation for small $B_0$, already visible for $B_0 = 0$, is attributed at this stage on the one hand to the overestimation of $\varphi(t)$ observed in [22], and on the other hand to an artefact due to the partial summation of the Dyson series.

At higher rigidity ($\rho = 1$), the Larmor radius of the particles is always larger than the eddy sizes and scatterings can be considered independent one from another. The process is Markovian and the decorrelation gets exponential in the pure turbulence case, as demonstrated in [9] based on a white-noise approximation to describe the 2-pt correlation function $\varphi(t)$. By increasing $B_0$, the decay of the decorrelations gets slower. Similarly to the case $\rho = 0.1$, the calculation is observed to underestimate the "decay time"; yet the values of $B_0$ leading to the underestimation span a much wider range.

The velocity decorrelation function relevant for the perpendicular diffusion corresponds to $i = j = x$ or $i = j = y$ in equation 14. The calculation proceeds the same way as for the parallel diffusion:

$$\hat{W}_{0x}(s) = \frac{1}{s} - \frac{\delta\Omega^2}{3}\frac{\hat{W}_{0x}(s)}{s}\mathcal{L}\left[\varphi(x)\left(1+\cos\Omega_0 x\right)\right](s), \tag{17}$$

and

$$\begin{aligned}\hat{W}_x(s) = {} & \frac{1}{s} - \frac{\delta\Omega^2}{3}\frac{\hat{W}_x(s)}{s}\mathcal{L}\left[\varphi(x)\langle w_x(x)\rangle_0(1+\cos\Omega_0 x)\right](s) \\ & + 2\left(\frac{\delta\Omega^2}{3}\right)^2\frac{\hat{W}_x(s)}{s}\mathcal{L}\left[\varphi(x_1+x2)\varphi(x_2+x3)\langle w_x(x_1)\rangle_0\langle w_x(x_2)\rangle_0\langle w_x(x_3)\rangle_0\cos^2\Omega_0\left(\frac{x_1}{2}+x_2+\frac{x_3}{2}\right)\right](s).\end{aligned} \tag{18}$$

The relevant decorrelation function is $\langle v_{0\perp} v_\perp(t)\rangle = \langle w_{0x} w_x(t)\rangle\cos\Omega_0 t = \langle w_{0y} w_y(t)\rangle\cos\Omega_0 t$.

A first illustration of the calculation is given in Fig. 2 (left panel), where the perpendicular decorrelation function is shown for $\rho = 0.1$ and $B_0 = 1$ μG. The dashed line is from Monte-Carlo simulations. As in the case of

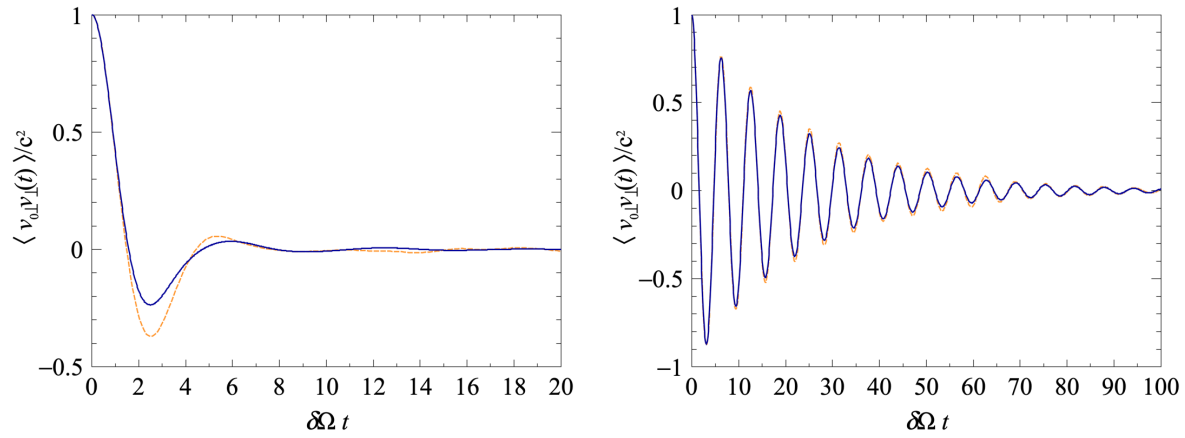


Figure 2: Perpendicular velocity decorrelation function of particles with reduced rigidity $\rho = 0.1$ (left) and $\rho = 1$ (right) for $\delta B = 1$ µG and $B_0 = 1$µG, as a function of the gyroperiod time scale $\delta\Omega t$. Dashed line is from Monte-Carlo simulations.

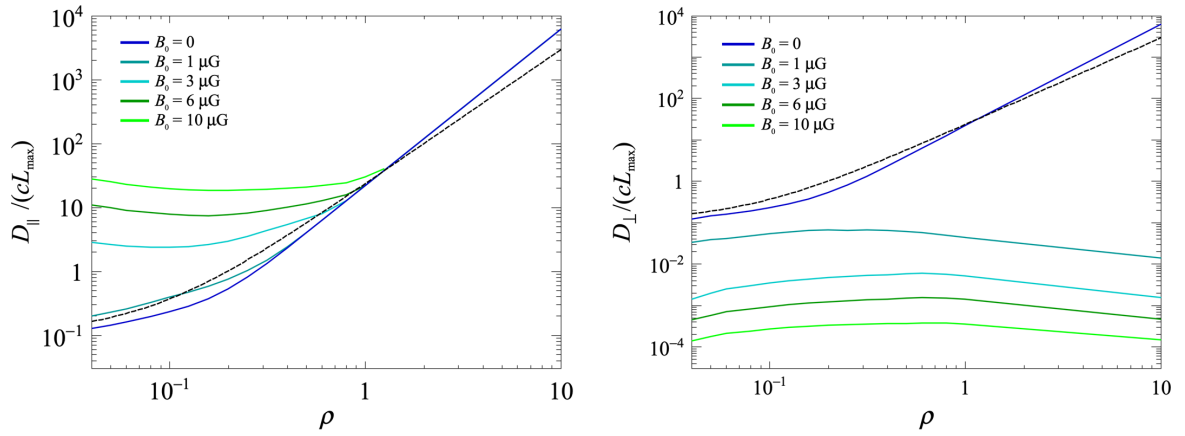


Figure 3: Parallel (left) and perpendicular (right) diffusion coefficient as a function of the reduced rigidity for different values of $B_0$ ($\delta B = 1$ µG). The Dashed line is from Monte-Carlo simulations in the pure turbulent case ($B_0 = 0$).

parallel diffusion, the envelope of the decay is slightly underestimated by the calculation. However, the modulations features, which have been shown from various simulations to be responsible for the perpendicular sub-diffusive regime at early times, are well reproduced. It is to be noted that none of the approximations proposed in the literature could predict both the fast decaying envelope and the positions of minimum and second maximum inherited from the modulations on top of the decay.

A second illustration is given in Fig. 2 , for $\rho = 0.1$ and $B_0 = 1$ µG. At such a high rigidity, the decay time scale is longer than the gyroperiod time scale $\Omega_0 t$, hence the numerous oscillations. The results from the calculation or from the simulations are almost indistinguishable.

The dependence in rigidity of the parallel diffusion coefficient $D_\parallel$ is shown in Fig. 3 (left panel) for different values of $B_0$, expressed in units of $cL_{\rm max}$. The dashed line displays, for reference, the results obtained from Monte-Carlo simulations in the case of pure turbulence. Despite the aforementioned differences between the simulations and the calculation, $D_\parallel$ is observed to be reproduced within a factor 2. In particular, the calculation slightly deviates from the expected scalings in $\rho^{1/3}$ in the gyroresonant regime an in $\rho^2$ in the quasi-ballistic regime [25, 26, 27]. As $B_0$ is increasing, from the analysis of the decorrelation functions presented above, $D_\parallel$ is expected to be more and more underestimated; yet the calculation presented here provides genuine qualitative scalings that are also reliable quantitatively around $\rho = 0.1$.

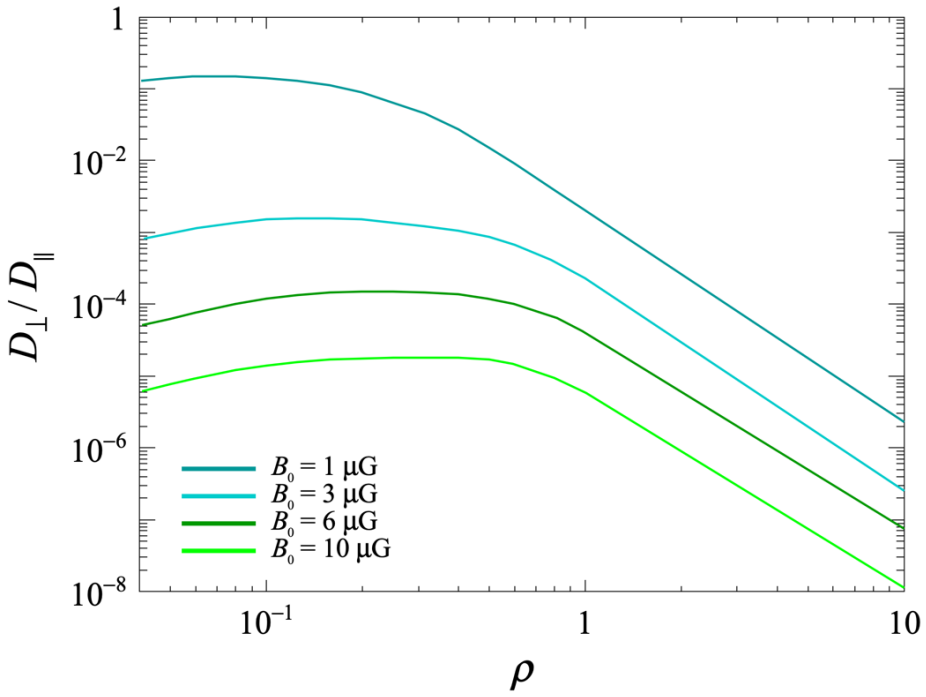


Figure 4: Ratio between perpendicular and parallel diffusion coefficient as a function of the reduced rigidity for different values of $B_0$ ($\delta B = 1$ μG).

In the same manner as in the parallel transport, the dependence in rigidity of the perpendicular diffusion coefficient $D_\perp$ is shown in Fig. 3 (right panel) for different values of $B_0$, expressed in units of $cL_{\rm max}$. Due to the oscillatory behavior of the velocity decorrelation functions, the additional time integration should smooth out differences between the simulations and the calculations. As $B_0$ is increasing, $D_\perp$ is decreasing, as expected (for $B_0 \to \infty$, a particle would be spiraling around $\mathbf{B}_0$ at a fixed radius). More revealing is the rigidity dependence of $D_\perp$, observed to rise more slowly than that of $D_\parallel$ in the gyroresonant regime and, unlike $D_\parallel$, to decrease in the high-rigidity regime. These dependencies are more clearly highlighted in Fig. 4, where the ratio $D_\perp/D_\parallel$ is displayed. The rise at low rigidities is in agreement with that revealed in Monte-Carlo studies in which the turbulence dynamical range well covers the rigidities of interest [17]. Furthermore, the decrease at high rigidities is also in agreement with these simulations, as is the shift of the transition region towards higher rigidities as $B_0$ is increasing.

In conclusion, velocity decorrelation functions of high-energy cosmic rays propagating in magnetic fields have been obtained from the Dyson series governing the motion of the particles. The particular example of Kolmogorov turbulence has been used, as it is a widely-used benchmark; yet there is a priori no restriction in the formalism to inject any spectrum of turbulence into Eqn. 5. The absence of small parameter of expansion forbids any perturbation theory to hold, and hence any truncation of the Dyson series [28]. The partial-summation scheme developed in this study is shown to provide an approximate solution that captures the main features uncovered by numerical simulations in a range of rigidities covering the transition between the gyroresonant and the quasi-ballistic regimes on the one hand, and the quasi-ballistic regime itself on the other hand. Keeping in mind the limitations underlined in terms of underestimation of the diffusion coefficients, the calculation based on Eqn. 14 provides a rapid tool for deriving approximate solutions without having to resort to heavy numerical simulation campaigns.

A key ingredient of the approximate solution relies on the modeling of the 2-pt correlation function of the turbulence experienced by the particles between two successive times. The approximation proposed in this study is found to reproduce the main features uncovered, here again, by numerical simulations as long as the reduced rigidity is larger than about one tenth of the largest scale of the turbulence. Progress in the modeling of this 2-pt function is needed to extend to lower rigidity the range of validity of the type of calculation presented in this study.

## References

[1] Kubo R 1957 J. Phys. Soc. Jap. **12** 570–586

[2] Giacalone J and Jokipii J R 1999 Astrophys. J. **520** 204–214

[3] Casse F, Lemoine M and Pelletier G 2001 Phys. Rev. D **65**(2) 023002 URL https://link.aps.org/doi/10.1103/PhysRevD.65.023002

[4] Candia J and Roulet E 2004 JCAP **10** 007 (*Preprint* astro-ph/0408054)

[5] Parizot E 2004 Nucl. Phys. B Proc. Suppl. **136** 169–178 (*Preprint* astro-ph/0409191)

[6] De Marco D, Blasi P and Stanev T 2007 Numerical Propagation of Cosmic Rays in the Galaxy 30th International Cosmic Ray Conference vol 2 pp 195–198 (*Preprint* 0705.3184)

[7] Globus N, Allard D and Parizot E 2008 Astron. Astrophys. **479** 97 (*Preprint* 0709.1541)

[8] Hauff T, Jenko F, Shalchi A and Schlickeiser R 2010 Astrophys. J. **711** 997–1007

[9] Plotnikov I, Pelletier G and Lemoine M 2011 Astron. Astrophys. **532** A68 (*Preprint* 1105.0618)

[10] Harari D, Mollerach S and Roulet E 2014 Phys. Rev. D **89** 123001 (*Preprint* 1312.1366)

[11] Fatuzzo M and Melia F 2014 Astrophys. J. **784** 131 (*Preprint* 1402.5469)

[12] Sonsrettee W, Subedi P, Ruffolo D, Matthaeus W H, Snodin A P, Wongpan P and Chuychai P 2015 Astrophys. J. **798** 59

[13] Snodin A P, Shukurov A, Sarson G R, Bushby P J and Rodrigues L F S 2016 Mon. Not. Roy. Astron. Soc. **457** 3975–3987 (*Preprint* 1509.03766)

[14] Subedi P et al. 2017 Astrophys. J. **837** 140 (*Preprint* 1612.09507)

[15] Giacinti G, Kachelriess M and Semikoz D V 2018 JCAP **07** 051 (*Preprint* 1710.08205)

[16] Reichherzer P, Becker Tjus J, Zweibel E G, Merten L and Pueschel M J 2020 Mon. Not. Roy. Astron. Soc. **498** 5051–5064 (*Preprint* 1910.07528)

[17] Dundovic A, Pezzi O, Blasi P, Evoli C and Matthaeus W H 2020 Phys. Rev. D **102** 103016 (*Preprint* 2007.09142)

[18] Reichherzer P, Merten L, Dörner J, Becker Tjus J, Pueschel M J and Zweibel E G 2022 Appl. Sciences **4** 15 (*Preprint* 2104.13093)

[19] Reichherzer P, Bott A F A, Ewart R J, Gregori G, Kempski P, Kunz M W and Schekochihin A A 2023 (*Preprint* 2311.01497)

[20] Deligny O 2021 Astrophys. J. **920** 87 (*Preprint* 2107.04391)

[21] Deligny O 2024 (*Preprint* 2406.00361)

[22] Deligny O, Reichherzer P and Schlegel L 2023 PoS **ICRC2023** 509

[23] Bourret R C 1962 Il Nuovo Cimento **XXVI** 3833

[24] Stehfest H 1970 Commun. ACM **13** 4749

[25] Wentzel D G 1974 Ann. Rev. Astron. Astrophys. **12** 71–96

[26] Bhattacharjee P and Sigl G 2000 Phys. Rept. **327** 109–247 (*Preprint* astro-ph/9811011)

[27] Aloisio R and Berezinsky V 2004 Astrophys. J. **612** 900–913 (*Preprint* astro-ph/0403095)

[28] Kraichnan R H 1961 Journal of Mathematical Physics **2** 124–148 ISSN 0022-2488 (print), 1089-7658 (electronic), 1527-2427 URL http://jmp.aip.org/resource/1/jmapaq/v2/i1/p124$_s$1